Temperature-dependent self-assembly of NC–Ph_5–CN molecules on Cu(111)

Marina Pivetta,[a] Giulia E. Pacchioni, Edgar Fernandes, and Harald Brune
Institute of Condensed Matter Physics, Ecole Polytechnique Fédérale de Lausanne (EPFL), CH-1015 Lausanne, Switzerland

(Received 8 December 2014; accepted 6 February 2015; published online 25 February 2015)

We present the results of temperature-dependent self-assembly of dicarbonitrile-pentaphenyl molecules (NC–Ph_5–CN) on Cu(111). Our low-temperature scanning tunneling microscopy study reveals the formation of metal-organic and purely organic structures, depending on the substrate temperature during deposition (160–300 K), which determines the availability of Cu adatoms at the surface. We use tip functionalization with CO to obtain submolecular resolution and image the coordination atoms, enabling unequivocal identification of metal-coordinated nodes and purely organic ones. Moreover, we discuss the somewhat surprising structure obtained for deposition and measurement at 300 K. © *2015 AIP Publishing LLC.* [http://dx.doi.org/10.1063/1.4909518]

I. INTRODUCTION

The spontaneous formation of organic structures and patterns on surfaces is a complex but fascinating process.[1–3] Self-assembled organic or metal-organic networks can be used as template for the adsorption of guest species[4,5] or for the growth of nanostructures in the network pores.[6] The self-assembly of metal-organic structures permits to obtain arrays of metal adatoms in a particular configuration exhibiting specific magnetic[7] or chemical[8] properties.

Using molecules containing functional (carboxyl,[9–11] thiol,[12] pyridyl,[13–15] carbonitrile[16–18]) groups capable of coordination with metal atoms (Fe, Co, Mn, Cu) gives the opportunity to create stable networks, since metal-organic bonds are expected to be stronger than those acting in purely organic assemblies.[1,3] However, in the absence of metal adatoms, the same functional groups can participate in the formation of hydrogen bonds.[9,19] Coordination bonds between Cu atoms and N-containing groups have been observed, e.g., for molecules comprising pyridyl groups co-deposited with Cu adatoms on HOPG[20,21] or Au(111).[14,22,23] At sufficiently high temperature, however, copper substrates can spontaneously supply adatoms for coordination, as reported for molecules containing pyridyl groups on Cu(100)[13,24] and on Cu(111).[15,25–27] On Cu(111), Cu coordination or hydrogen bond formation occurs depending on deposition temperature for a N-substituted derivative of pyrene,[28,29] for molecules containing pyridyl groups,[26] and for a carbonitrile-modified anthracene species.[17] The question whether the molecules may play an active role in the atom detachment from steps has emerged.[18,28] Also, the influence of the deposition rate on the assembly outcome was investigated for trinitrile molecules.[18]

On Ag(111), dicarbonitrile-polyphenyls (NC–Ph_n–CN, with $n = 3 - 6$) and Co adatoms form metal-organic honeycomb networks.[16,30] In the absence of Co adatoms, the same molecules self-assemble into purely organic structures with different symmetries.[19,31,32] Recently, we have shown that similar honeycomb patterns form on Cu(111) by taking advantage of the two-dimensional gas of Cu adatoms present at the surface.[6] Such networks have been used as template for the self-assembly of metal cluster arrays nucleating on the network components[33] or in the network pores.[6]

Here, we show how the self-organization of dicarbonitrile-pentaphenyl (NC–Ph_5–CN) molecules on Cu(111) depends on substrate temperature during deposition, in particular on the availability of Cu adatoms at the surface. Upon cooling after deposition at T_{dep} = 300 K, twofold coordination bonds form between carbonitrile groups and Cu adatoms, giving rise to chains. We deduce that coordination two is preferred as long as the molecular density is sufficiently low to allow enough lateral distance between the chains. Coordination three, observed for deposition of the same amount of molecules at T_{dep} = 250 K, leads to the formation of a highly regular honeycomb network. Lowering the substrate temperature to T_{dep} = 220 K reduces the Cu adatom density, yielding to a hitherto unobserved assembly phase stabilized by alternating metal coordination and hydrogen bonds. At even lower temperatures (T_{dep} = 160 K), the Cu adatoms are absent and the dicarbonitrile-pentaphenyl molecules form purely organic hydrogen-bonded networks of various symmetries. Furthermore, we show a compact, Cu-coordinated structure obtained for deposition and measurement at room temperature (RT). We discuss the role of possible interactions in the stabilization of such different assemblies.

II. EXPERIMENTAL

The Cu(111) substrate was prepared by Ar^+ sputtering (2 $\mu A/cm^2$, 800 eV, 20 min) and annealing (800 K, 20 min) cycles. The NC–Ph_5–CN molecules[16] were synthesized by Ruben and collaborators (Forschungszentrum Karlsruhe, Germany) and evaporated from a molecular effusion cell at 230 °C. We used substrate temperatures during deposition, T_{dep}, ranging from 300 to 160 K; during each preparation, T_{dep} was constant.

[a]Electronic mail: marina.pivetta@epfl.ch

As we will see in what follows, there are many structures that form as a function of the deposition temperature and some of them can coexist. Each reported value of T_{dep} was chosen in order to maximize the abundance of one single structure. All the measurements were carried out with a low temperature scanning tunneling microscope (STM) at 5 K, except for the data shown in Fig. 10, which were acquired at RT.[34] The STM images were recorded in constant current mode, the indicated bias voltages V_t correspond to the sample potential. High resolution measurements were carried out by functionalizing the STM tip with a CO molecule.[35–37]

The molecular coverage (monolayer (ML)) is defined in terms of the densest structure we have observed, i.e., the compact structure formed at room temperature reported in Sec. III E. The evaporation flux and the deposition time, and therefore the molecular exposure, are identical for each preparation. Assuming that the sticking coefficient does not depend on the substrate temperature, each deposition corresponds to 0.4 ± 0.1 ML.

III. RESULTS AND DISCUSSION

A. Chains

Figure 1 shows a STM image of a sample prepared by evaporating the NC–Ph_5–CN molecules at T_{dep} = 300 K. The molecules assemble into a homogeneous layer of equally spaced parallel chains. At this coverage, the average distance between chains is 3 ± 1 nm. As expected, this structure has three rotational domains, and the Fast Fourier Transform (FFT) confirms that they differ by 120°. The chain directions are close to the second nearest neighbor directions, $\langle 11\bar{2}\rangle$. Some of the chains split in two branches through threefold arrangements and very few of them form closed structures.

In Fig. 2(a), we show a high-resolution image of the one-dimensional assemblies and of the split threefold structures. We obtained this image by functionalizing the STM tip with a CO molecule in order to enhance the resolution.[35–37] Contrary to images obtained with standard tips, submolecular details are displayed and the Cu coordination atoms are visible, appearing as dim protrusions between the molecules.[38] Most of the molecules are parallel to one of the $\langle 11\bar{2}\rangle$ directions. Only three of them, enclosed by white lines and labeled from 1 to 3, are aligned along directions that are clearly different from the $\langle 11\bar{2}\rangle$ ones. Molecules 1 and 2 are aligned along the nearest neighbor directions $\langle 1\bar{1}0\rangle$, while molecule 3 deviates from all high symmetry directions. Even in their straight sections, however, the chains are wavy. In Fig. 2(b), also acquired with the functionalized tip but at lower tunneling voltage, it is possible to recognize the five rings composing the molecules and the Cu coordination atom; moreover, one can see that two consecutive molecules are not perfectly aligned: each molecule points straight to a Cu atom at one end, while at the other end there is a lateral misalignment between endgroup and adatom. This geometry is sketched in Fig. 2(c). The wavy appearance of the chains is explained by the existence of two equivalent positions (left or right) for the adatom at the non-aligned end, see scheme in Fig. 2(d), and consequently also

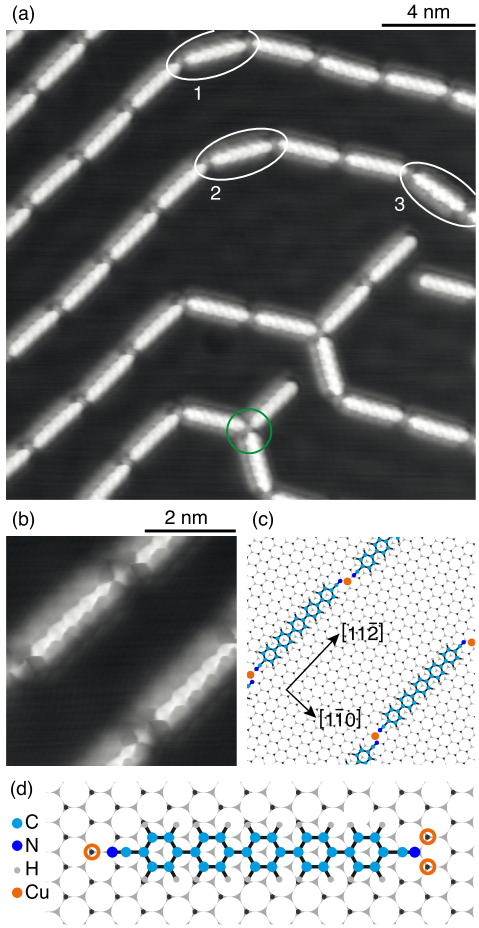

FIG. 2. (a) STM image of the chains (T_{dep} = 300 K, T_{STM} = 5 K, 20×20 nm^2, V_t = −5 mV, I_t = 20 pA). 1, 2, and 3 indicate molecules that deviate from $\langle 11\bar{2}\rangle$. Green circle surrounds a threefold node. (b) STM image of the nodes (5×5 nm^2, V_t = −2 mV, I_t = 20 pA). (c) Model of (b). (d) Model showing that the left end of the molecule is, along the molecular axis, at the right distance from a fcc site that can be occupied by a Cu adatom. On the right end, the axially aligned fcc site is further away from the terminal N atom, while there are two equivalent off-axis sites that are closer to the molecule endgroup. The Cu coordination adatom occupies one of these two sites.

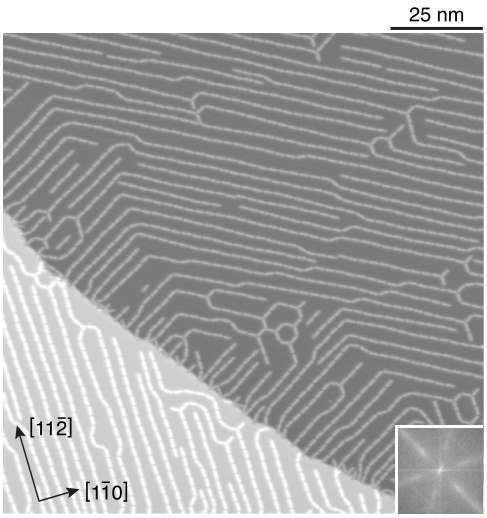

FIG. 1. STM image of chain domains (T_{dep} = 300 K, T_{STM} = 5 K, 130×130 nm^2, V_t = −0.2 V, I_t = 20 pA). Inset: FFT of a larger STM image showing the three orientational domains.

for the following molecule. In Sec. III B, we discuss in more detail this behavior, i.e., the formation of coordination nodes in which the carbonitrile groups do not point straight to the adatom. In our model, we propose that the Cu coordination atoms occupy fcc hollow sites.[39] The molecules are aligned along $\langle 11\bar{2}\rangle$ directions, and the phenyl rings are centered over hcp hollow sites with threefold orientation, a favorable configuration for benzene adsorption on Cu(111).[40,41] Notice that the distance between consecutive phenyl rings (441 pm, deduced from the gas-phase structure[16]) and the distance between two Cu atoms in this direction ($a\sqrt{3}$ = 444 pm, with a = 256 pm the distance between nearest neighbors on the Cu(111) surface[42]) differ by only 0.4%. This coincidence allows all phenyl rings to occupy equivalent sites. The nitrogen atoms occupy hollow sites, a geometry which was reported on Ag(111) to be favorable,[31] but not exclusive.[30,32] The projected Cu-N bond length deduced from the STM data and from the model is 190 ± 20 pm, in agreement with values reported for double and triple CN-coordinated Cu adatoms, where a small out of plane component was reported.[17,18]

The formation of these metal-organic chains requires the presence of a sufficiently high amount of Cu adatoms at the surface. The adatom concentration results from an equilibrium between detachment and attachment processes from kink sites, and depends on the temperature, on the energy barrier for detachment and diffusion, and on the step and kink density. Formation of Cu-coordinated bonds for deposition[12,15,18,25,43] or annealing[17,28] at room temperature has been reported for several kinds of molecules on Cu(111).

By considering the average distance between the chains, this self-assembled structure corresponds to a maximum adatom density of 6×10^{-3} ML. The energy required for the formation of an adatom, owing to atom detachment from a kink and diffusion on the terrace, has been determined experimentally from Cu adatom island decay (0.78 ± 0.04 eV)[44] and from temperature dependent step fluctuations (0.76 ± 0.15 eV).[45] These values are in agreement with the result of 0.85 eV obtained by density functional theory calculations.[46] For the attempt frequency, a pre-exponential factor $\nu_0 = 1.6 \times 10^{10\pm1.7}$ s^{-1} has been reported,[45] lower than the typical value of 10^{12} s^{-1} usually considered for these processes.[47] These parameters hint towards rather low adatom concentration at room temperature. Nevertheless, if we take into account a kink density of 1×10^{-3} ML, consistent with our data for the Cu(111) substrate, the deposition time (300 s), and the time before the sample is cooled (approximately ten minutes), we find with the parameters reported by Giesen[45] an adatom density of the order of 3×10^{-3} ML at room temperature. For comparison, with the energy barrier of 0.78 ± 0.04 eV[44] and $\nu_0 = 10^{12}$ s^{-1}, we obtain an adatom density of 8×10^{-2} ML. Therefore, if we consider that the molecules break the adatom evaporation/condensation equilibrium by trapping the Cu adatoms, this estimation indicates that for our system at T_{dep} = 300 K, it is not necessary to invoke an active role of the molecules in detaching the atoms from the step edges to obtain the adatom density required for the coordination nodes.

The fact that the chains do not deviate too much from the high symmetry directions is likely due to a lateral repulsion between the molecules. The existence of such a long-range interaction is in agreement with the two following observations: (i) For lower coverage, the chains are further apart from each other. (ii) For higher coverage, a different assembly where the Cu atoms are coordinated by three molecules, the honeycomb network, obtained also by lowering the deposition temperature, is observed (see Sec. III B). An interaction driven by a charge transfer from/to the substrate can be the origin of the repulsion between the chains, as already reported for other one dimensional molecular systems.[25,48–50] A surface state mediated interaction, observed for different adatoms on Cu(111)[51,52] or for pentacene molecules on Cu(110),[53] seems not to be pertinent here, since we find a coverage-dependent average distance between the chains.

A few examples of coordination three, giving rise to chain splitting, see green circle in Fig. 2(a), are already observed on this sample. We will show in Sec. III B that the threefold coordination is the building block of the honeycomb structure, obtained for deposition at 250 K, or for deposition of a slightly higher amount of molecules at RT. This observation is in line with the one reported for molecules containing three pyridyl groups: twofold coordination is more favorable, but threefold coordination, allowing a denser structure, takes place for higher molecular coverage,[22] although for similar systems the preference for twofold coordination was interpreted as due to geometric constraints or steric hindrance.[13,25]

We deduce that for our system, coordination two is preferred below a certain coverage, for which the molecules can form chains that are far enough from each other, and as long as it is allowed by the ratio between the density of molecules and of adatoms.

B. Honeycomb

Deposition at T_{dep} = 250 K leads to the formation of a honeycomb network, as shown in Fig. 3(a). Two substrate terraces, separated by a monoatomic step, are covered by two disconnected domains; one dimensional structures as in Fig. 1 develop from the domain borders towards the Cu(111) step edge. This is another indication that in proximity of the step edges, especially on the lower terrace, the Cu adatom concentration is higher and that coordination two is preferred. The STM image and its FFT pattern shown in Fig. 3(b) demonstrate that the two domains have different orientations with respect to the substrate. We define the orientation of a honeycomb domain as one of the three equivalent directions in which hexagons are adjacent (see red and blue lines). From the analysis of more than one hundred different domains, two preferred orientations differing by 5.2° ± 0.6° are clearly identified, see Fig. 3(c). They correspond to +2.5° ± 0.6° (right orientation) and −2.7° ± 0.7° (left orientation) with respect to the crystallographic $\langle 1\bar{1}0\rangle$ directions. We deduce the network periodicity, corresponding to the distance between two parallel molecules of a given hexagon, to be 4.97 ± 0.04 nm.

Figure 4(a) shows a STM image acquired on a domain with left orientation: the Cu coordination atoms are visible and submolecular details of the linkers are displayed. Figure 4(b) presents a closeup view also acquired with the functionalized tip, but at lower bias voltage: the five phenyl rings of each molecule are resolved, as well as the Cu atoms. While the node

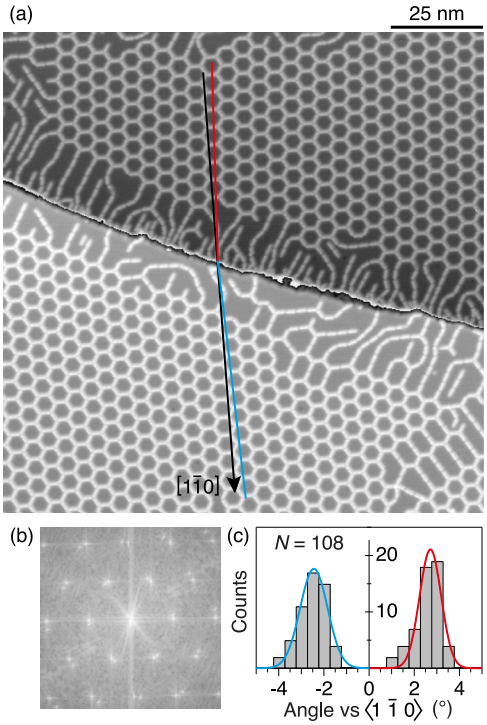

FIG. 3. (a) STM image showing two honeycomb rotational domains on two adjacent Cu(111) terraces separated by a monoatomic step (T_{dep} = 250 K, T_{STM} = 5 K, 130×130 nm^2, V_t = −0.25 V, I_t = 20 pA). (b) FFT of the STM image in (a). (c) Histogram of orientations of the honeycomb domains with respect to ⟨1$\bar{1}$0⟩ and gaussian fit to the data.

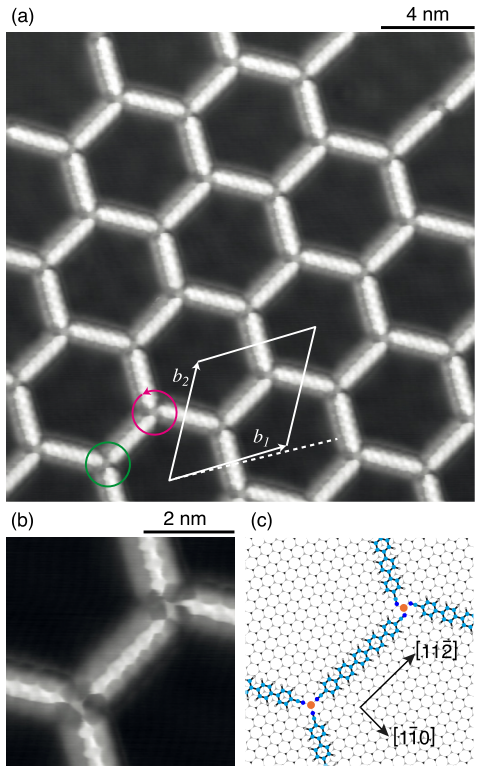

FIG. 4. (a) STM image of a honeycomb domain with left orientation (T_{dep} = 250 K, T_{STM} = 5 K, 20×20 nm^2, V_t = −5 mV, I_t = 20 pA). Green circle: aligned node; magenta circle: rotated node. Dotted line: ⟨1$\bar{1}$0⟩ direction, $\boldsymbol{b}_1$ and $\boldsymbol{b}_2$: unit cell vectors. (b) STM image of the two types of nodes (5×5 nm^2, V_t = −2 mV, I_t = 20 pA). (c) Structure model of (b).

in the lower part of the image appears symmetric, in the other one, the molecular endgroups do not point straight towards the Cu atom, see Fig. 2(d), yielding a counterclockwise-rotated node. We can therefore identify two types of nodes: aligned ones, green circle in Fig. 4(a), and rotated ones, magenta circle, alternating at the corners of the hexagons. In Fig. 4(c), we present the corresponding model, which is build coherently with the geometry presented in Fig. 2(d), but with threefold symmetry, with molecules aligned along three distinct ⟨11$\bar{2}$⟩ directions. It accounts for all the experimental observations, as the network periodicity and the existence of two orientational domains: domains with right orientation can be described by considering that in the rotated nodes, the Cu adatom occupies the fcc site on the other side of the endgroups, and consequently the molecules present a clockwise arrangement around it. For the left orientation, the unit cell structure in terms of the Cu(111) unit cell vectors $\boldsymbol{a}_1$ (along [1$\bar{1}$0]) and $\boldsymbol{a}_2$ (along [0$\bar{1}$1]) is given in matrix notation by

$$\begin{pmatrix} \boldsymbol{b}_1 \\ \boldsymbol{b}_2 \end{pmatrix} = \begin{pmatrix} 19 & 1 \\ -1 & 20 \end{pmatrix} \begin{pmatrix} \boldsymbol{a}_1 \\ \boldsymbol{a}_2 \end{pmatrix}.$$

The unit cells, $\boldsymbol{b}_1$ and $\boldsymbol{b}_2$, and a ⟨1$\bar{1}$0⟩ direction are sketched in Fig. 4(a). The model yields $b = |\boldsymbol{b}_1| = |\boldsymbol{b}_2| = 4.99$ nm and angles of ±2.54° with respect to ⟨1$\bar{1}$0⟩, in very good agreement with the experimental values. The network has a (NC–Ph$_5$–CN)$_3$Cu$_2$ stoichiometry.

The model corresponds to an adatom density of 5.2 × 10^{-3} ML, slightly lower than the one required for the formation of the chains described in Sec. III A. These values are in agreement with the fact that, for the same amount of molecules, lowering T_{dep} from room temperature to 250 K leads to assembly into honeycomb domains.

Notice that in the STM image shown in Fig. 4(b), the chemical bonds between the CN groups and the Cu coordination atoms are visible.[36] The CN-Cu bonds are imaged as bright connections between the endgroup and the coordination atom in a darker circular halo, slightly distorted in the case of the rotated node, surrounding the Cu atoms.

On Ag(111), subsequent deposition of NC–Ph$_5$–CN molecules and Co leads to the formation of a honeycomb network similar to the one reported here.[16] In that case, coordination between ligands is ensured by Co atoms; in their absence, a purely organic kagome network is formed.[19] The (NC–Ph$_5$–CN)$_3$Co$_2$ honeycomb lattice formed on Ag(111) is less regular than the one observed here, which presents perfect long-range order although the cavities are not regular hexagons because of the rotated nodes. On Ag(111), the molecules point straight towards the Co atom in all the nodes, but significative deviations from the ideal value of 120° were reported for the angle between molecules. In general, on Ag(111), NC–Ph$_n$–CN molecules coordinate to different metal adatoms by forming aligned nodes, as for Co[16,30] or lanthanides.[54] Recently Sirtl *et al.* have described the assembly of trinitrile molecules on Cu(111).[18] In that case, a honeycomb structure is formed by coordination two to Cu adatoms. The authors have reported the formation of a tilted node, that they tentatively explain with the presence of a Cu dimer instead of a single atom. This interpretation, however, does not apply to our system,

neither for the twofold nor for the threefold rotated nodes, since it yields a bent geometry that does not correspond to our observations.

Our results show the coexistence of aligned threefold nodes and nodes where the three carbonitrile groups do not point straight towards the Cu atom. In a different experiment (not shown), we have observed that in the presence of Co adatoms on Cu(111), the NC–Ph_5–CN molecules coordinate to Co rather than to Cu. Preference for other transition metal adatoms with respect to Cu has been reported for molecules containing pyridyl groups, forming more stable bonds with Fe adatoms than with Cu.[14,55] The Co-coordinated honeycomb structure has the same characteristics as the (NC-Ph_5-CN)$_3$$Cu_2$ one, i.e., alternating aligned and rotated nodes that confer a chiral character to the network. Therefore we deduce that the decisive elements for the formation of the observed honeycomb network are the epitaxy of the NC–Ph_5–CN molecules on Cu(111) and the resulting molecule-substrate interaction energy, which prevails over the preference for a straight node geometry. This is in agreement with the fact that on Ag(111), where there is no match between phenyl-phenyl distance and substrate lattice, only aligned nodes were observed.[16,30] Notice however that different results can be expected for shorter polyphenyls, since in that case the contribution of the molecule-substrate interaction to the total energy is smaller.

C. Truncated triangles

For deposition at T_{dep} = 220 K, the NC–Ph_5–CN self-assemble in a network with cavities having a truncated-triangle shape, as shown in Fig. 5(a). Regions of bare substrate are visible, indicating that this phase has a higher molecular density. Inspection of the STM image and of its FFT pattern shown in Fig. 5(b) demonstrates that also this structure exhibits rotational domains. Although the shape of the cavities is unusual, also this network presents a very high degree of long-range order. The result of the statistical analysis of the observed orientations is shown in Fig. 5(c): two preferred orientations differing by 17.2° ± 0.8° are deduced, corresponding to 8.6° ± 0.9° and −8.5° ± 0.8° with respect to ⟨1$\bar{1}$0⟩. For this network, we find a periodicity of 4.53 ± 0.03 nm.

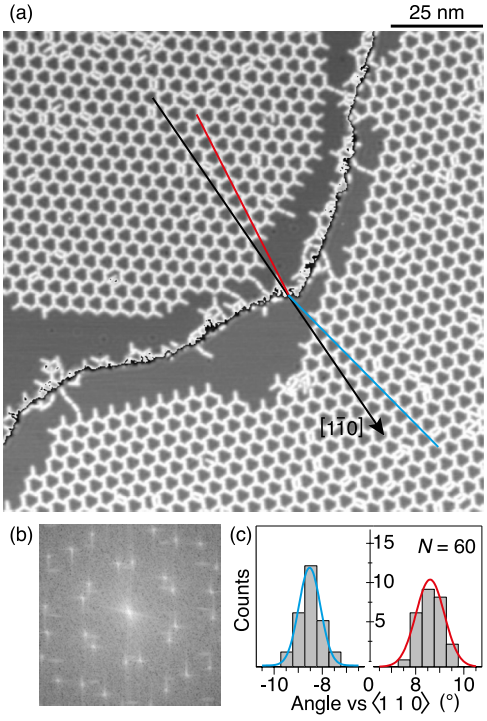

FIG. 5. (a) STM image showing rotational domains of the truncated-triangle network on two Cu(111) terraces separated by a step (T_{dep} = 220 K, T_{STM} = 5 K, 130×130 nm^2, V_t = −0.25 V, I_t = 20 pA). (b) FFT of the STM image in (a). (c) Histogram of the orientation of the domains with respect to ⟨1$\bar{1}$0⟩ and gaussian fit to the data.

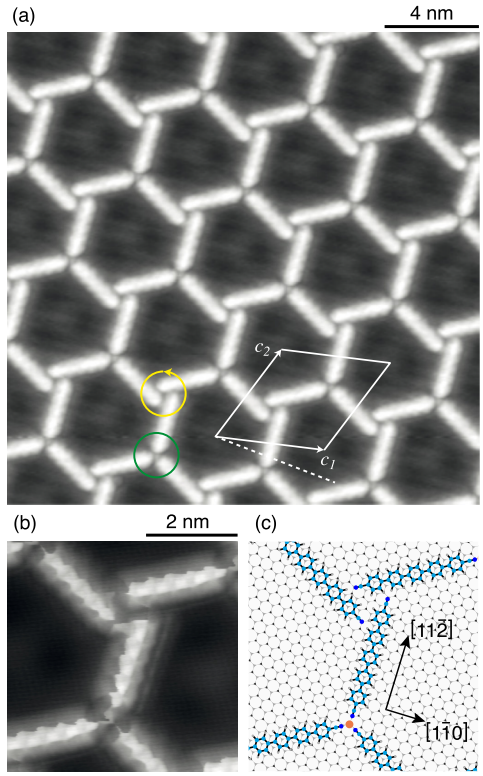

FIG. 6. (a) STM image of a truncated-triangle domain with left orientation (T_{dep} = 220 K, T_{STM} = 5 K, 20×20 nm^2, V_t = −20 mV, I_t = 20 pA). Green circle: aligned node; yellow circle: rotated node. Dotted line: ⟨1$\bar{1}$0⟩ direction, $\boldsymbol{c}_1$ and $\boldsymbol{c}_2$: unit cell vectors. (b) STM image of the two types of nodes (5×5 nm^2, V_t = −2 mV, I_t = 20 pA). (c) Structure model of (b).

In Figure 6(a), we show a STM image acquired on a truncated-triangle network domain with left orientation. For this lattice, the difference between the two types of nodes is evident already at the first glance. The node enclosed by the green circle is the aligned node already observed in the honeycomb structure, with the Cu atom visible as small bright dot. The node marked by the yellow circle, with the endgroup pointing toward the side of the other molecule, is clearly chiral with a counterclockwise rotation and is formed without coordination atom. The two nodes alternate at the corners of the truncated triangles. Figure 6(b) shows an image acquired at lower bias, confirming the absence of Cu atom in the rotated node. Moreover, the formation of hydrogen bonds between CN and HC groups is detected. In Fig. 6(c), we present the model describing the structure of the truncated-triangular network: as for the honeycomb network, the molecules are adsorbed along ⟨11$\bar{2}$⟩, and the Cu atoms occupy fcc sites. The unit cell can be represented in matrix notation in terms of the Cu(111) unit cell

vectors $\boldsymbol{a}_1$ and $\boldsymbol{a}_2$ as

$$\begin{pmatrix} \boldsymbol{c}_1 \\ \boldsymbol{c}_2 \end{pmatrix} = \begin{pmatrix} 16 & 3 \\ -3 & 19 \end{pmatrix} \begin{pmatrix} \boldsymbol{a}_1 \\ \boldsymbol{a}_2 \end{pmatrix}.$$

The unit cells, $\boldsymbol{c}_1$ and $\boldsymbol{c}_2$, and the $[1\bar{1}0]$ direction are sketched in Fig. 6(a). The model yields $c = 4.52$ nm and angles of ±8.44° with respect to $\langle 1\bar{1}0 \rangle$, in good agreement with the measured values. The domains with right orientation are described by the same model, but with clockwise rotated nodes. This network has a $(\text{NC-Ph}_5\text{-CN})_3\text{Cu}_1$ stoichiometry.

Pawin *et al.* described a phase formed by carbonitrile-modified antracene molecules on Cu(111) at intermediate temperature, where the Cu adatom density is too low to ensure the formation of the fully coordinated phase.[17] Recently, the formation of complex structures formed by tripodal molecules containing pyridyl groups and Cu coordination atoms on a Ag(111) surface was observed, where both Cu-pyridyl and pyridyl-HC linkages are present.[27,56] Our result, however, is the first observation of a regular network of cavities with alternating metal-coordinated and hydrogen-bonded nodes. For NC–Ph_3–CN on Ag(111), in case of under-stoichiometric Co deposition, the coexistence of honeycomb domains and purely organic assemblies has been reported.[32] Therefore, the alternation of metal-coordinated nodes and purely organic ones characterizing the truncated-triangle network is typical for the coordination with Cu atoms.

D. Kagome and triangles

Further lowering of T_{dep} to 160 K leads to the formation of purely molecular assemblies. Figure 7 shows typical examples of such structures. The two islands are formed by smaller patches of different patterns, linked by transition regions. Among them, it is possible to recognize a kagome motif and some hexagonal patterns. The fact that these structures coexist points towards similar formation energies.[31] Some additional molecules, also linked via hydrogen bonds, are present in the larger cavities,[16,19] leading to denser regions. From the rotation of the nodes, we deduce that in each of the two domains, all the assemblies possess the same handedness, as also confirmed by the FFT of each domain shown as insets. The two domains have opposite chirality: left (counterclockwise orientation) for the assembly in the upper part of the image, right (clockwise orientation) for the other one. The periodicity of the kagome structure is 5.11 ± 0.03 nm.

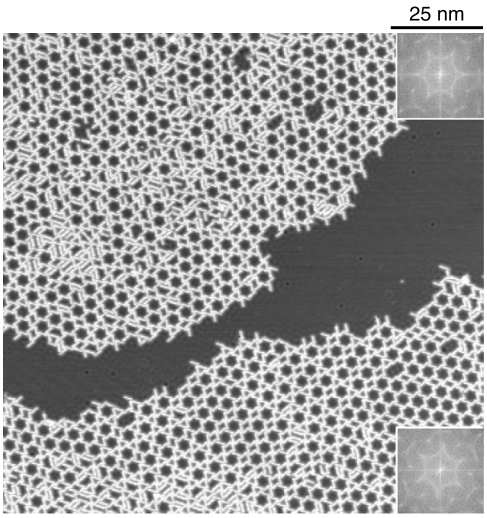

FIG. 7. STM image showing two domains of purely organic assemblies ($T_{\text{dep}} = 160$ K, $T_{\text{STM}} = 5$ K, 130×130 nm^2, $V_t = -0.1$ V, $I_t = 20$ pA). Inset in the upper (lower) corner: FFT of the domain in the upper (lower) part of the image.

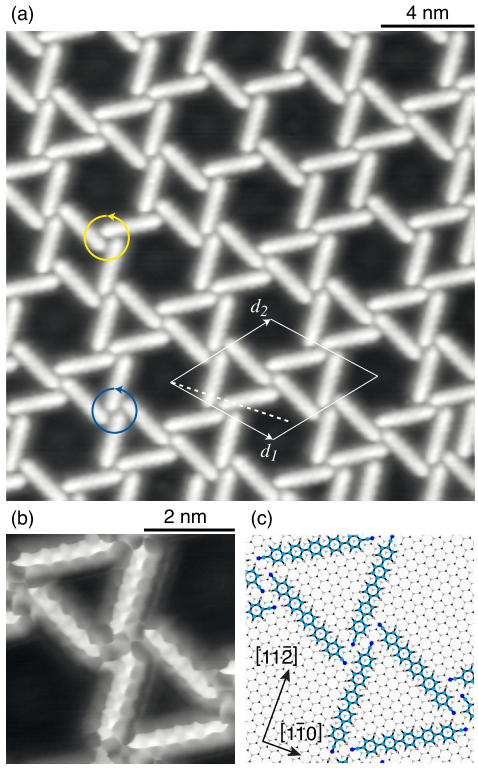

FIG. 8. (a) STM image of a kagome domain with left orientation ($T_{\text{dep}} = 160$ K, $T_{\text{STM}} = 5$ K, 20×20 nm^2, $V_t = -20$ mV, $I_t = 20$ pA). Blue circle: fourfold node; yellow circle: rotated threefold node. Dotted line: $\langle 1\bar{1}0 \rangle$ direction, $\boldsymbol{d}_1$ and $\boldsymbol{d}_2$: unit cell vectors. (b) Closeup view of the fourfold node (5×5 nm^2, $V_t = -2$ mV, $I_t = 20$ pA). (c) Model relative to (b).

Figure 8(a) shows a closeup view of the molecular assembly. In this region, we find nodes constituted by the junction of four molecules (blue circle), leading to the formation of the kagome pattern. Nodes formed by three molecules as in the truncated-triangular network, yellow circle, are also present and constitute defects in the kagome pattern. Figure 8(b) shows the detail of the kagome intermolecular bonds, obtained by using a functionalized tip. In each node, the four molecules are arranged in a geometry promoting the formation of several H–NC bonds. We describe this motif with a model in which all the NC–Ph_5–CN molecules are adsorbed along the $\langle 11\bar{2} \rangle$ directions, see Fig. 8(c). The kagome structure is represented in matrix notation in terms of the Cu(111) unit cell vectors $\boldsymbol{a}_1$ and $\boldsymbol{a}_2$ as

$$\begin{pmatrix} \boldsymbol{d}_1 \\ \boldsymbol{d}_2 \end{pmatrix} = \begin{pmatrix} 22 & -5 \\ 5 & 17 \end{pmatrix} \begin{pmatrix} \boldsymbol{a}_1 \\ \boldsymbol{a}_2 \end{pmatrix}$$

with $d = 5.10$ nm, in agreement with the experimental value.

A kagome pattern was already reported for deposition of NC–Ph_5–CN on Ag(111).[19] In that case, the authors observed

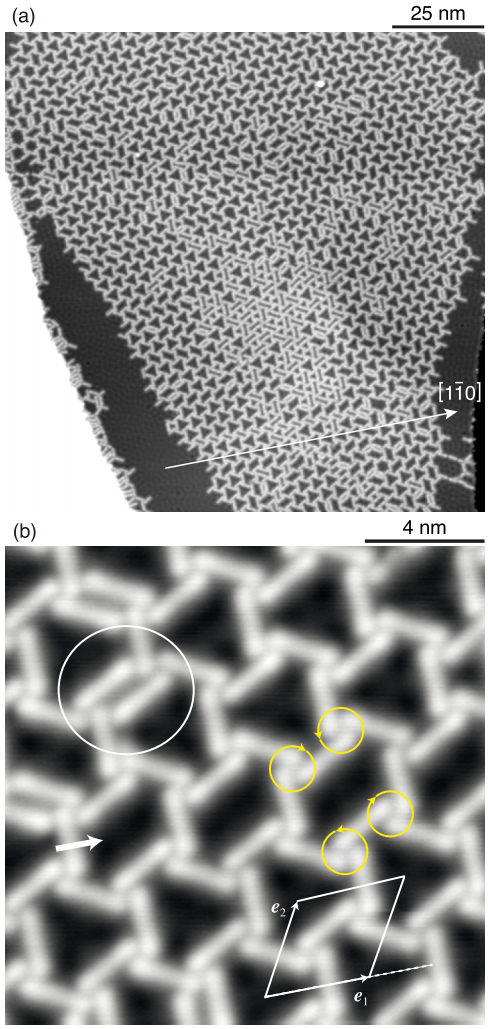

FIG. 9. (a) STM image of a domain of the triangular network (T_{dep} = 160 K, T_{STM} = 5 K, 130×130 nm^2, V_t = −20 mV, I_t = 20 pA). (b) Closeup view: a row of rhombi, inducing a boundary between two differently oriented regions, is indicated by the arrow. Yellow circles: threefold nodes; large white circle encloses a typical defect. Dotted line: ⟨1$\bar{1}$0⟩, $\boldsymbol{e}_1$ and $\boldsymbol{e}_2$ are the unit cell vectors. (T_{dep} = 160 K, T_{STM} = 5 K, 16×16 nm^2, V_t = −20 mV, I_t = 20 pA).

two slightly different types of nodes formed by the junction of four molecules, originating from a non-planar adsorption of the molecules together with the stacking on the Ag(111) surface. The observation of only one type of node for the kagome network formed by NC–Ph$_6$–CN on Ag(111) was attributed to a more planar adsorption configuration.[31] For our system, in the kagome pattern, only one type of node is identified, indicating a planar adsorption geometry which is likely the same for all the self-assembled structures observed at low-temperature.

In Fig. 9(a), we show a second phase observed together with the kagome one, formed by triangles and rhombi. The central part of the island appears denser because of additional molecules hosted in the cavities, as for the kagome pattern. Adjacent triangles are aligned along ⟨1$\bar{1}$0⟩. The periodicity of this network is 3.84 ± 0.03 nm. Figure 9(b) presents a closeup view of this network. The triangles are composed of nodes, as the ones of the truncated-triangle phase. Here, however, in each triangle, nodes of opposite handedness alternate. The rhombi appear as defects which induce a change in the orientation of the triangles (upper part of the image: triangles pointing up, lower part: triangles pointing down). Another type of imperfection is enclosed by the white circle: two opposite nodes are not well aligned and induce the formation of triangles with the opposite orientation. Overall, this phase is not chiral. The regular triangular structure (discarding the presence of the rhombi) can be represented in matrix notation in terms of $\boldsymbol{a}_1$ and $\boldsymbol{a}_2$, with e = 3.83 nm

$$\begin{pmatrix} \boldsymbol{e}_1 \\ \boldsymbol{e}_2 \end{pmatrix} = \begin{pmatrix} 15 & 0 \\ 0 & 15 \end{pmatrix} \begin{pmatrix} \boldsymbol{a}_1 \\ \boldsymbol{a}_2 \end{pmatrix}.$$

The formation of purely organic assemblies at T_{dep} = 160 K reflects the fact that at this temperature, the adatom density is extremely low. We still observe the formation of some metal-organic nodes, or the decoration of steps by short chains, but the overall adatom density is negligible.

E. Compact

Deposition and imaging at 300 K leads to a much denser molecular structure than the chains spaced far apart presented in Sec. III A. The molecules form a compact structure composed of parallel chains, as shown in Fig. 10. The structure is rather unstable and very sensitive to the tunneling parameters, for example, it was impossible to obtain STM images with negative bias voltage. Notice that the sample was not completely covered by molecules, i.e., regions of bare Cu(111) substrate were present. The regular parts of the assembly have a rectangular unit cell with periodicity of 2.8 ± 0.2 nm along, and 1.3 ± 0.1 nm perpendicular to the chains. We use this dense structure to define a molecular ML: knowing the Cu(111) lattice parameter, 1 ML corresponds to one molecule per 64 substrate atoms.

These chains have the same periodicity along the chain direction as the ones shown in Sec. III A, for which we have unambiguously demonstrated the presence of Cu coordination atoms. Therefore we deduce that the molecules are axially coordinated to Cu atoms. This interpretation is supported by the comparison with the dense-packed structure reported for

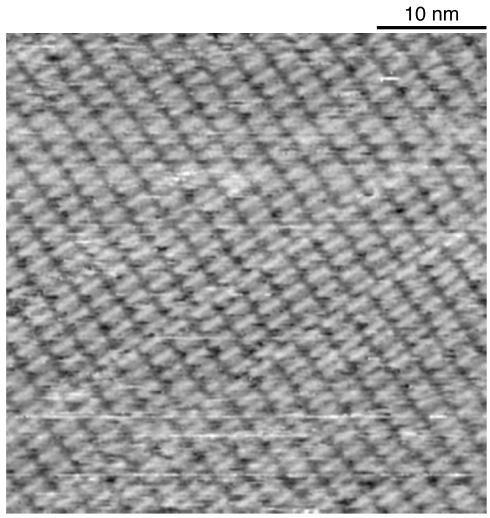

FIG. 10. STM image of a compact domain (T_{dep} = 300 K, T_{STM} = 300 K, 45×45 nm^2, V_t = +1.4 V, I_t = 100 pA).

TABLE I. Summary of the characteristics of the observed self-assembled structures.

Structure	T_{dep} (K)	T_{STM} (K)	Unit cell area (Cu unit cell)	Molecules: Per unit cell	Molecules: (ML)	Cu adatoms: Per unit cell	Cu adatoms: Coordination
Chains	300	5	-	-	<0.36	-	2
Honeycomb	250	5	381	3	0.51	2	3
Truncated-triangular	220	5	313	3	0.61	1	3
Kagome	160	5	399	6	0.96	0	-
Triangular	160	5	225	3	0.85	0	-
Compact	300	300	64	1	1	1	2

NC–Ph_6–CN on Ag(111).[31] In fact, in the absence of coordination atoms as for the case on Ag(111), the molecules form a dense structure in which the molecules are not aligned, but the CN groups interdigitate, in line with the fact that two CN groups repel each other.

The formation of this compact structure at 300 K indicates that at this temperature, the prevailing interactions are not the ones leading to the formation of the chains homogeneously covering the surface observed after cooling the sample, see Sec. III A. The fact that the molecules are found laterally close to each other likely reflects a different origin for the binding to the surface. It is also possible that at room temperature, some degrees of freedom, such as the tilting of the phenyl rings with respect to each other, are present, while they are inhibited at low temperature.

IV. CONCLUSIONS

We have shown that, depending on the substrate temperature during deposition, NC–Ph_5–CN molecules form on Cu(111) different metal-organic and purely organic structures, as summarized in Table I. Our results indicate that metal coordination is ensured by the adatom gas created by the thermally activated atom detachment from kink sites. In fact, the overall assembly behavior as a function of the deposition temperature demonstrates that for lower temperature, there are less adatoms available.

The common feature of all the regular structures observed at T_{STM} = 5 K is the orientation of the NC–Ph_5–CN molecules along the $\langle 11\bar{2} \rangle$ directions of the Cu(111) surface. The epitaxial match between Cu(111) and polyphenyl chain certainly plays a role in inducing this preferential adsorption geometry. Moreover, this configuration maximizes the number of nitrogen atoms occupying favorable adsorption sites.

ACKNOWLEDGMENTS

We acknowledge M. Ruben, S. Klyatskaya, and J. V. Barth for providing us with the organic molecules, and the Swiss National Science Foundation for financial support.

[1]J. V. Barth, "Molecular architectonic on metal surfaces," Annu. Rev. Phys. Chem. **58**, 375 (2007).
[2]T. Kudernac, S. B. Lei, J. A. A. W. Elemans, and S. De Feyter, "Two-dimensional supramolecular self-assembly: Nanoporous networks on surfaces," Chem. Soc. Rev. **38**, 402 (2009).
[3]L. Bartels, "Tailoring molecular layers at metal surfaces," Nat. Chem. **2**, 87 (2010).
[4]M. Stöhr, M. Wahl, H. Spillmann, L. H. Gade, and T. A. Jung, "Lateral manipulation for the positioning of molecular guests within the confinements of a highly stable self-assembled organic surface network," Small **3**, 1336 (2007).
[5]Z. Cheng, J. Wyrick, M. Luo, D. Sun, D. Kim, Y. Zhu, W. Lu, K. Kim, T. L. Einstein, and L. Bartels, "Adsorbates in a box: Titration of substrate electronic states," Phys. Rev. Lett. **105**, 066104 (2010).
[6]M. Pivetta, G. E. Pacchioni, U. Schlickum, J. V. Barth, and H. Brune, "Formation of Fe cluster superlattice in a metal-organic quantum-box network," Phys. Rev. Lett. **110**, 086102 (2013).
[7]P. Gambardella, S. Stepanow, A. Dmitriev, J. Honolka, F. M. F. de Groot, M. Lingenfelder, S. Sen Gupta, D. D. Sarma, P. Bencok, S. Stanescu, S. Clair, S. Pons, N. Lin, A. P. Seitsonen, H. Brune, J. V. Barth, and K. Kern, "Supramolecular control of the magnetic anisotropy in two-dimensional high-spin Fe arrays at a metal interface," Nat. Mater. **8**, 189 (2009).
[8]D. Grumelli, B. Wurster, S. Stepanow, and K. Kern, "Bio-inspired nanocatalysts for the oxygen reduction reaction," Nat. Commun. **4**, 2904 (2013).
[9]J. V. Barth, J. Weckesser, N. Lin, A. Dmitriev, and K. Kern, "Supramolecular architectures and nanostructures at metal surfaces," Appl. Phys. A **76**, 645 (2003).
[10]T. Classen, M. Lingenfelder, Y. Wang, R. Chopra, C. Virojanadara, U. Starke, G. Costantini, G. Fratesi, S. Fabris, S. de Gironcoli, S. Baroni, S. Haq, R. Raval, and K. Kern, "Hydrogen and coordination bonding supramolecular structures of trimesic acid on Cu(110)," J. Phys. Chem. A **111**, 12589 (2007).
[11]Y.-F. Zhang, N. Zhu, and T. Komeda, "Mn-coordinated stillbenedicarboxylic ligand supramolecule regulated by the herringbone reconstruction of Au(111)," J. Phys. Chem. C **111**, 16946 (2007).
[12]H. Walch, J. Dienstmaier, G. Eder, R. Gutzler, S. Schlögl, T. Sirtl, K. Das, M. Schmittel, and M. Lackinger, "Extended two-dimensional metal-organic frameworks based on thiolate-copper coordination bonds," J. Am. Chem. Soc. **133**, 7909 (2011).
[13]S. L. Tait, A. Langner, N. Lin, S. Stepanow, C. Rajadurai, M. Ruben, and K. Kern, "One-dimensional self-assembled molecular chains on Cu(100): Interplay between surface-assisted coordination chemistry and substrate commensurability," J. Phys. Chem. C **111**, 10982 (2007).
[14]Z. L. Shi, J. Liu, T. Lin, F. Xia, P. N. Liu, and N. Lin, "Thermodynamics and selectivity of two-dimensional metallo-supramolecular self-assembly resolved at molecular scale," J. Am. Chem. Soc. **133**, 6150 (2011).
[15]T. R. Umbach, M. Bernien, C. F. Hermanns, L. L. Sun, H. Mohrmann, K. E. Hermann, A. Krüger, N. Krane, Z. Yang, F. Nickel, Y.-M. Chang, K. J. Franke, J. I. Pascual, and W. Kuch, "Site-specific bonding of copper adatoms to pyridine end groups mediating the formation of two-dimensional coordination networks on metal surfaces," Phys. Rev. B **89**, 235409 (2014).
[16]U. Schlickum, R. Decker, F. Klappenberger, G. Zoppellaro, S. Klyatskaya, M. Ruben, I. Silanes, A. Arnau, K. Kern, H. Brune, and J. V. Barth, "Metal-organic honeycomb nanomeshes with tunable cavity size," Nano Lett. **7**, 3813 (2007).
[17]G. Pawin, K. L. Wong, D. Kim, D. Sun, L. Bartels, S. Hong, T. S. Rahman, R. Carp, and M. Marsella, "A surface coordination network based on substrate-derived metal adatoms with local charge excess," Angew. Chem., Int. Ed. **47**, 8442 (2008).
[18]T. Sirtl, S. Schlögl, A. Rastgoo-Lahrood, J. Jelic, S. Neogi, M. Schmittel, W. M. Heckl, K. Reuter, and M. Lackinger, "Control of intermolecular bonds by deposition rates at room temperature: Hydrogen bonds versus metal coordination in trinitrile monolayers," J. Am. Chem. Soc. **135**, 691 (2013).

[19]U. Schlickum, R. Decker, F. Klappenberger, G. Zoppellaro, S. Klyatskaya, W. Auwärter, S. Neppl, K. Kern, H. Brune, M. Ruben, and J. V. Barth, "Chiral kagome lattice from simple ditopic molecular bricks," J. Am. Chem. Soc. **130**, 11778 (2008).
[20]A. Breitruck, H. E. Hoster, C. Meier, U. Ziener, and R. J. Behm, "Interaction of Cu atoms with ordered 2D oligopyridine networks," Surf. Sci. **601**, 4200 (2007).
[21]A. Breitruck, H. E. Hoster, and R. J. Behm, "Short-range order in a metal-organic network," J. Phys. Chem. C **113**, 21265 (2009).
[22]J. Liu, T. Lin, Z. Shi, F. Xia, L. Dong, P. N. Liu, and N. Lin, "Structural transformation of two-dimensional metal-organic coordination networks driven by intrinsic in-plane compression," J. Am. Chem. Soc. **133**, 18760 (2011).
[23]Z. L. Shi, T. Lin, J. Liu, P. N. Liu, and N. Lin, "Regulating a two-dimensional metallo-supramolecular self-assembly of multiple outputs," CrystEngComm **13**, 5532 (2011).
[24]A. Langner, S. L. Tait, N. Lin, R. Chandrasekar, M. Ruben, and K. Kern, "Ordering and stabilization of metal-organic coordination chains by hierarchical assembly through hydrogen bonding at a surface," Angew. Chem., Int. Ed. **47**, 8835 (2008).
[25]D. Heim, D. Ecija, K. Seutert, W. Auwärter, C. Aurisicchio, C. Fabbro, D. Bonifazi, and J. V. Barth, "Self-assembly of flexible one-dimensional coordination polymers on metal surfaces," J. Am. Chem. Soc. **132**, 6783 (2010).
[26]W. H. Wang, S. Y. Wang, Y. N. Hong, B. Z. Tang, and N. Lin, "Selective supramolecular assembly of multifunctional ligands on a Cu(111) surface: Metallacycles, propeller trimers and linear chains," Chem. Commun. **47**, 10073 (2011).
[27]D. Ecija, S. Vijayaraghavan, W. Auwärter, S. Joshi, K. Seufert, C. Aurisicchio, D. Bonifazi, and J. V. Barth, "Two-dimensional short-range disordered crystalline networks from flexible molecular modules," ACS Nano **6**, 4258 (2012).
[28]M. Matena, M. Stöhr, T. Riehm, J. Björk, S. Martens, M. S. Dyer, M. Persson, J. Lobo-Checa, K. Müller, M. Enache, H. Wadepohl, J. Zegenhagen, T. A. Jung, and L. H. Gade, "Aggregation and contingent metal/surface reactivity of 1,3,8,10-tetraazaperopyrene (TAPP) on Cu(111)," Chem. Eur. J. **16**, 2079 (2010).
[29]J. Björk, M. Matena, M. S. Dyer, M. Enache, J. Lobo-Checa, L. H. Gade, T. A. Jung, M. Stöhr, and M. Persson, "STM fingerprint of molecule-adatom interactions in a self-assembled metal-organic surface coordination network on Cu(111)," Phys. Chem. Chem. Phys. **12**, 8815 (2010).
[30]D. Kühne, F. Klappenberger, R. Decker, U. Schlickum, H. Brune, S. Klyatskaya, M. Ruben, and J. V. Barth, "High-quality 2D metal-organic coordination network providing giant cavities within mesoscale domains," J. Am. Chem. Soc. **131**, 3881 (2009).
[31]D. Kühne, F. Klappenberger, R. Decker, U. Schlickum, H. Brune, S. Klyatskaya, M. Ruben, and J. V. Barth, "Self-assembly of nanoporous chiral networks with varying symmetry from sexiphenyl-dicarbonitrile on Ag(111)," J. Phys. Chem. C **113**, 17851 (2009).
[32]U. Schlickum, F. Klappenberger, R. Decker, G. Zoppellaro, S. Klyatskaya, M. Ruben, K. Kern, H. Brune, and J. V. Barth, "Surface-confined metal-organic nanostructures from Co-directed assembly of linear terphenyl-dicarbonitrile linkers on Ag(111)," J. Phys. Chem. C **114**, 15602 (2010).
[33]R. Decker, U. Schlickum, F. Klappenberger, G. Zoppellaro, S. Klyatskaya, M. Ruben, J. V. Barth, and H. Brune, "Using metal-organic templates to steer the growth of Fe and Co nanoclusters," Appl. Phys. Lett. **93**, 243102 (2008).
[34]R. Gaisch, J. K. Gimzewski, B. Reihl, R. R. Schlittler, M. Tschudy, and W. D. Schneider, "Low-temperature ultra-high vacuum scanning tunneling microscope," Ultramicroscopy **42–44**, 1621 (1992).
[35]C. Weiss, C. Wagner, C. Kleimann, M. Rohlfing, F. S. Tautz, and R. Temirov, "Imaging Pauli repulsion in scanning tunneling microscopy," Phys. Rev. Lett. **105**, 086103 (2010).
[36]C. Weiss, C. Wagner, R. Temirov, and F. S. Tautz, "Direct imaging of intermolecular bonds in scanning tunneling microscopy," J. Am. Chem. Soc. **132**, 11864 (2010).
[37]G. Kichin, C. Weiss, C. Wagner, F. S. Tautz, and R. Temirov, "Single molecule and single atom sensors for atomic resolution imaging of chemically complex surfaces," J. Am. Chem. Soc. **133**, 16847 (2011).
[38]This functionalized tip generates a shadow on the left-hand side of the imaged structures, but this does not prevent the identification of the phenyl rings and of the Cu coordination atoms.
[39]J. Repp, G. Meyer, K.-H. Rieder, and P. Hyldgaard, "Site determination and thermally assisted tunneling in homogenous nucleation," Phys. Rev. Lett. **91**, 206102 (2003).
[40]T. S. Chwee and M. B. Sullivan, "Adsorption studies of C_6H_6 on Cu(111), Ag(111), and Au(111) within dispersion corrected density functional theory," J. Chem. Phys. **137**, 134703 (2012).
[41]W. Reckien, M. Eggers, and T. Bredow, "Theoretical study of the adsorption of benzene on coinage metals," Beilstein J. Org. Chem. **10**, 1775 (2014).
[42]N. W. Ashcroft and N. D. Mermin, *Solid State Physics* (Saunders College, 1976).
[43]W. H. Wang, Y. N. Hong, X. G. Shi, C. Minot, M. A. Van Hove, B. Z. Tang, and N. Lin, "Inspecting metal-coordination-induced perturbation of molecular ligand orbitals at a submolecular resolution," J. Phys. Chem. Lett. **1**, 2295 (2010).
[44]G. Schulze Icking-Konert, M. Giesen, and H. Ibach, "Decay of Cu adatom islands on Cu(111)," Surf. Sci. **398**, 37 (1998).
[45]M. Giesen, "Scaling transition of the time dependence of step fluctuations on Cu(111)," Surf. Sci. **442**, 543 (1999).
[46]P. J. Feibelman, "Formation and diffusion of S-decorated Cu clusters on Cu(111)," Phys. Rev. Lett. **985**, 606 (2000).
[47]R. Gomer, "Diffusion of adsorbates on metal surfaces," Rep. Prog. Phys. **53**, 917 (1990).
[48]G. Tomba, M. Stengel, W.-D. Schneider, A. Baldereschi, and A. De Vita, "Supramolecular self-assembly driven by electrostatic repulsion: The 1D aggregation of rubrene pentagons on Au(111)," ACS Nano **4**, 7545 (2010).
[49]J. V. Barth, J. Weckesser, C. Cai, P. Günter, L. Bürgi, O. Jeandupeux, and K. Kern, "Building supramolecular nanostructures at surfaces by hydrogen bonding," Angew. Chem., Int. Ed. **39**, 1230 (2000).
[50]J. Fraxedas, S. García-Gil, S. Monturet, N. Lorente, I. Fernández-Torrente, K. J. Franke, J. I. Pascual, A. Vollmer, R.-P. Blum, N. Koch, and P. Ordejón, "Modulation of surface charge transfer through competing long-range repulsive versus short-range attractive interactions," J. Phys. Chem. C **115**, 18640 (2011).
[51]J. Repp, F. Moresco, G. Meyer, K. H. Rieder, P. Hyldgaard, and M. Persson, "Substrate mediated long-range oscillatory interaction between adatoms: Cu/Cu(111)," Phys. Rev. Lett. **85**, 2981 (2000).
[52]N. Knorr, H. Brune, M. Epple, A. Hirstein, M. A. Schneider, and K. Kern, "Long-range adsorbate interactions mediated by a two-dimensional electrons gas," Phys. Rev. B **65**, 115420 (2002).
[53]S. Lukas, G. Witte, and C. Wöll, "Novel mechanism for molecular self-assembly on metal substrates: Unidirectional rows of pentacene on Cu(110) produced by a substrate-mediated repulsion," Phys. Rev. Lett. **88**, 028301 (2001).
[54]J. I. Urgel, D. Ecija, W. Auwärter, A. C. Papageorgiou, A. P. Seitsonen, S. Vijayaraghavan, S. Joshi, S. Fischer, J. Reichert, and J. V. Barth, "Five-vertex lanthanide coordination on surfaces: A route to sophisticated nanoarchitectures and tessellations," J. Phys. Chem. C **118**, 12908 (2014).
[55]A. Langner, S. L. Tait, N. Lin, R. Chandrasekar, V. Meded, K. Fink, M. Ruben, and K. Kern, "Selective coordination bonding in metallo-supramolecular systems on surfaces," Angew. Chem., Int. Ed. **51**, 4327 (2012).
[56]S. Vijayaraghavan, D. Ecija, W. Auwärter, S. Joshi, K. Seufert, M. Drach, D. Nieckarz, P. Szabelski, C. Aurisicchio, D. Bonifazi, and J. V. Barth, "Supramolecular assembly of interfacial nanoporous networks with simultaneous expression of metalorganic and organic-bonding motifs," Chem. Eur. J. **19**, 14143 (2013).